ACS APPLIED MATERIALS & INTERFACES

Research Article

Cite This: ACS Appl. Mater. Interfaces 2018, 10, 35547−35556

www.acsami.org

All-Organic Conductive Biomaterial as an Electroactive Cell Interface

Ao Zhuang,[†] Yongjun Bian,[†,‡] Jianwei Zhou,[†] Suna Fan,[†] Huili Shao,[†] Xuechao Hu,[†] Bo Zhu,*[,‡] and Yaopeng Zhang*[,†]

[†]State Key Laboratory for Modification of Chemical Fibers and Polymer Materials, College of Materials Science and Engineering, Donghua University, Shanghai 201620, China

[‡]School of Materials Science and Engineering, Shanghai University, Shanghai 200444, China

Supporting Information

ABSTRACT: Various attractive materials are being used in bioelectronics recently. In this paper, hydroxymethyl-3,4-ethylenedioxythiophene (EDOT-OH) has been in situ integrated and polymerized on the surface of the regenerated silk fibroin (RSF) film to construct a biocompatible electrode. In order to improve the efficiency of in situ polymerization, sodium dodecyl sulfate (SDS) was adopted as surfactant to construct a well-organized and stable poly(hydroxymethyl-3,4-ethylenedioxythiophene) (PEDOT-OH) coating, whereas ammonium persulfate was used as oxidant. The effects of dosages of surfactant and oxidant, initial pH value, and monomer concentration on the polymerization were studied. Under the optimal conditions, the RSF/PEDOT-OH film exhibited a square resistance of 3.28×10^5 Ω corresponding to a conductance of 6.1×10^{-3} S/cm. Scanning electron microscope images indicated that PEDOT-OH was deposited uniformly on the surface of the RSF film with SDS. Furthermore, Fourier transform infrared spectroscopy confirmed that interactions existed between the peptide linkages of silk fibroin (SF) macromolecules and PEDOT-OH. The RSF/PEDOT-OH film displayed favorable electrochemical stability, biocompatibility, and fastness. This study provides a feasible method to endow conductivity to RSF materials in various forms. In addition, the conductive layer and biocompatible silk substrate make the RSF/PEDOT-OH biomaterial highly suitable for potential applications in bioelectric devices, sensors, and tissue engineering.

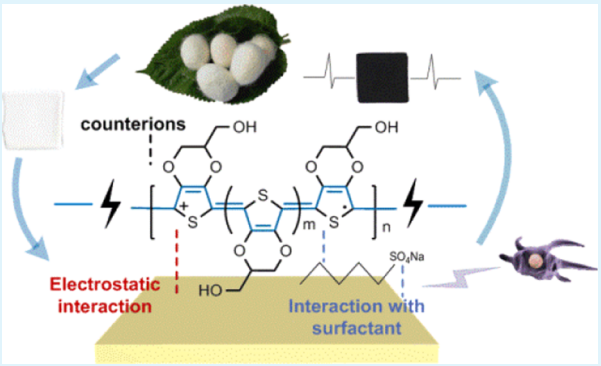

KEYWORDS: *regenerated silk fibroin, conductive biopolymer, in situ chemical oxidant polymerization, poly(hydroxymethyl-3,4-ethylenedioxythiophene), bioelectric devices*

1. INTRODUCTION

Bioelectronics, which integrates (bio)materials and circuits, represents a promising new field and opens new perspectives for numerous biomedical applications such as neural prostheses,[1−3] artificial muscles,[4] or biointegrated devices for biological signal detection and recording.[5−7] Silk fibroin can be considered as an interesting biomaterial for the preparation of implanted bioelectronics because of its flexibility, biocompatibility, and biodegradability.[8−23]

Silk fibers are composed of two fibroin monofilaments surrounded by sericin. The monofilament is made up of bundles of nanofibrils, which interact with each other and orient themselves parallel to the fiber axis. The sericin is normally removed by some degumming procedures as it prevents the penetration of dye liquor and induces a strong immune response. A clean removal of sericin exposes the nanofibrillar structure.[24−26] Extensive studies have been performed to modify the natural silks toward their potential applications in bioengineering. A major area of interest is focused on combining conductive polymers (CPs) with silks to construct electroactive composites, as the electrical signals could stimulate tissue regeneration and tune the delivery of drugs, genes, and growth factors.[13−16,21−23] Compared to inorganic and metal conductive materials, the mechanical properties of CP are more comparable with the extracellular matrix, which makes CPs more likely to meet the combined demands of electrical communication,[27,28] biocompatibility,[29,30] and mechanical strength[31,32] for implanted electronics. Both the solution coating and in situ polymerization of CPs were demonstrated to be efficient approaches to functionalize the natural silks by coating a CP layer on the fibers. The regenerated silk fibroin (RSF) materials are more versatile than the natural silks, as they are water-soluble and compatible with a series of solution processes (solution coating, inject printing, 3D printing, etc.). The shape and structure of RSF materials could be arbitrarily designed and well defined by these solution-processing approaches to match the request for implants or tissue scaffolds.[33−35] It is of great interest to add

Received: August 12, 2018
Accepted: September 20, 2018
Published: September 20, 2018

DOI: 10.1021/acsami.8b13820
ACS Appl. Mater. Interfaces 2018, 10, 35547−35556

a CP layer onto RSF materials to make them electroactive. Some previous studies have reported methods for depositing a polypyrrole (Ppy) or polyaniline (Pani) coating on RSF materials.[8,9,11,19,20]

Compared to other CPs, PEDOT shows better redox stability in biological environments,[36] more outstanding transparency in its oxidized state,[37] a high charge injection limit, and low potential excursion,[38] all of which benefit its further applications. In addition, the interfacial impedance of PEDOT at 1 kHz is relatively low, even less than that of Pt[28] and iridium oxide.[39] The abovementioned features ensure that PEDOT can provide stable and efficient charge delivery to attach cells/tissues, and indicate its potential in the bioelectronics field. In comparison with EDOT, EDOT-OH has been reported to have better solubility and lower onset oxidation potential in electrical polymerization.[40−43] Moreover, the ease of chemical functionalization of EDOT-OH makes it superior to EDOT, and its further functionalization could endow the electronic material with smart/selective functions directed to proteins, cells, and biomolecules.

On the basis of the above background, we consider it important to assemble an electroactive RSF material by integrating a poly(hydroxymethyl-3,4-ethylenedioxythiophene) (PEDOT-OH) layer on the RSF material. We initially attempted the coating approaches reported in previous works on the natural silks, including the physical coating of PEDOT:PSS followed by electrodeposition of PEDOT-OH, and direct oxidative deposition of PEDOT-OH. The former failed to introduce a strong interface adhesion and the PEDOT:PSS coating layer was delaminated by gentle water washing. The latter could only deposit an unstable and nonhomogeneous PEDOT-OH layer of poor conductivity on the RSF material. Other researchers have reported a method to electrochemically deposit PEDOT or PEDOT-OH on RSF which was first modified by a Ppy coating, and have successfully fabricated an RSF film and mat with better conductivity.[10,12] Nevertheless, the electrochemical polymerization technology of the CP has stricter demands for the substrate and environment. Compared to the above electrochemical method, the biomaterials modified by the simpler chemical oxidative method have obvious advantages for mass production, although the conductivity of the product is lower than that modified by electrochemical polymerization. However, it still remains a challenge to achieve a uniform and strong adhesion between the RSF materials and PEDOT or its derivatives by in situ chemical oxidative polymerization. A plausible explanation for this is that the RSF materials lack the fibrillar structure present in the degummed natural silks.[44] Toward this challenge, we developed a surfactant-aided oxidative deposition approach to fabricate PEDOT-OH-coated RSF materials. In aqueous solution, sodium dodecyl sulfate (SDS) molecules form micelles to encapsulate PEDOT-OHs and stabilize their dispersion.[40,41] This prevents PEDOT-OH molecules from aggregating and precipitating, and makes PEDOT-OH active for a long time for deposition on RSF materials. Moreover, SDS can enhance the interface adhesion of RSF materials with PEDOT-OH because of its intrinsic amphiphilicity. The as-prepared PEDOT-OH coatings on RSF, compared to those without SDS, were much superior in terms of uniformity, conductivity, and tunability of thickness. The PEDOT-OH-coated RSF further demonstrated its electroactivity as an electrode, stronger interface adhesion than the electropolymerized film, and excellent biocompatibility intrinsically derived from PEDOT-OH. We envision that the integration of the aforementioned attractive features would make this electroactive PEDOT-OH-coated RSF material a promising candidate for various in vitro and in vivo applications such as tissue engineering and artificial organs.

2. MATERIALS AND METHODS

2.1. Materials. *Bombyx mori* cocoons were produced in Tongxiang, China. Cellulose-semipermeable membranes with a molecular weight cutoff of 14 000 ± 2000 Da were purchased from Yuanju Co., Ltd., China.The gold plate was purchased from Suzhou Jingxi Electric Technology Co., Ltd. EDOT-OH was custom-synthesized. Lithium bromide (Shanghai Zhongli Industrial Co., Ltd., Shanghai, China), anhydrous sodium carbonate (Lingfeng Chemical Reagent Co., Ltd., Shanghai, China), SDS (Sangon Biotech Co. Ltd., Shanghai, China), ammonium persulfate (APS, Sinopharm Chemical Reagent Co., Ltd., Shanghai, China), hydrochloric acid (36.5%) (Pinghu Chemical Reagent Factory, Zhejiang, China), acetonitrile (Lingfeng Chemical Reagent Co., Ltd., Shanghai, China), anhydrous lithium perchlorate (Shanghai Aladdin Biochemical Technology Co., Ltd.), phosphate buffer saline (PBS) (Biosharp Co., Ltd.), Roswell Park Memorial Institute (RPMI) 1640 medium (Hyclone), horse serum (Gibco), fetal bovine serum (FBS) (Sigma), and nerve growth factor (NGF) (Invitrogen, Shanghai, China) were all used as received.

2.2. Preparation of the RSF Solution. Silkworm cocoons were cut and boiled in 0.5 wt % Na_2CO_3 solution for 30 min twice to remove sericin. After drying, the degummed silk was then dissolved in 9.0 M LiBr aqueous solution at 40 °C for 2 h, and dialyzed against deionized water for 3 days. After the RSF aqueous solution was concentrated to 20 wt % by forced air flow, glycerol was added to improve the formability of the RSF solution with a glycerol/RSF mass ratio of 5/100. The solution was stored at 4 °C for further use.

2.3. Preparation of an Insoluble RSF Film. To prepare a solid RSF film, 300 μL of the RSF/glycerol solution was pipetted on a square glass coverslip with a length of 2.4 cm, followed by overnight drying. Then, the film was soaked in 80% ethanol for 2 h to make the film insoluble in water. After rinsing with deionized water, the film was dried at room temperature for more than 24 h and then peeled off from the coverslip.

2.4. Preparation of the RSF/PEDOT-OH Composite Conductive Film by in Situ Chemical Oxidative Polymerization. The RSF film (2.4 cm × 2.4 cm × 0.0125 cm, 0.065 ± 0.005 g) was dispersed in PEDOT-OH aqueous solution (6.5 mL) containing SDS, and shaken in an incubator shaker at 30 °C for 30 min with a speed of 100 rpm. $(NH_4)_2S_2O_8$ was then added as an initiator of the polymerization. Hydrochloric acid solution (36.5 wt %) was used to adjust the pH value. After 24 h reaction with shaking, the film was washed by deionized water and sonicated for 40 s to remove any unstable polymer adsorbed on the surface of the RSF film. The RSF/PEDOT-OH film was then sandwiched between two glass coverslips to avoid shrinkage during drying at room temperature.

2.5. Electrical Conductance Measurements. The square resistance (R_s) was measured with a Keithley 236 Sourcemeter using a four-point probe. The film was first cut into rectangular strips (2 cm × 0.5 cm). Then, the four probes were arranged at the center of the film in a line along the long side direction. The distance between the two adjacent probes was 0.5 cm. R_s (Ω) was calculated by the equation $R_s = V/I$, where I is the applied current (A) and V is the resulting potential (V). Five measurements were taken and averaged for each data point. Thickness (H) of the conductive layers was obtained by evaluating the cross-sectional scanning electron microscope (SEM) images of the film. The conductance of the film was calculated according to the equation $\sigma = 1/(H \cdot R_s)$.[8]

2.6. Fourier Transform Infrared Spectroscopy. The influence of various factors on the structure of the as-prepared film was investigated by Fourier transform infrared (FTIR) spectroscopy. RSF films treated by pure water and by SDS acid solution and PEDOT-OH polymerized in water were used as the control samples to

DOI: 10.1021/acsami.8b13820
ACS Appl. Mater. Interfaces 2018, 10, 35547−35556

compare with RSF/PEDOT-OH films. The hydration process parameters were kept similar to those of polymerization (pH = 0.6, 30 °C, 24 h, 100 rpm). Furthermore, the RSF/PEDOT film was also fabricated under the same conditions as the RSF/PEDOT-OH film. All the films were characterized using a Nicolet 8700 spectrometer equipped with an attenuated total reflectance (ATR) accessory, whereas SDS, RSF treated by acid, and pure PEDOT-OH were also tested by transmission technology with KBr. FTIR spectra were recorded in the range of 2000−500 cm^{-1} by accumulating 64 scans at a resolution of 4 cm^{-1}.

2.7. Morphology Observation. Morphology of the film surface was observed by SEM (Hitachi SU8010). Samples were mounted onto specimen stubs by means of conductive double-sided adhesive tape and sputter-coated with a thin gold layer. The cross sections of the films were characterized by using a JEOL JSM-5600LV microscope. Samples were adhered on specimen stubs using conductive double-sided adhesive tape. To expose the conductive coating of the RSF/PEDOT-OH film, no gold or carbon layer was sputter-coated on the film.[8]

2.8. Electrochemical Characterization. Electrochemical stability of the representative RSF/PEDOT-OH film [modified at 30 mM monomer concentration, n(surfactant)/n(monomer) = 0.4, n(oxidant)/n(monomer) = 1.25, initial pH = 0.6] was evaluated by subjecting the films to oxidation and reduction cycles using cyclic voltammetry (CV). The RSF/PEDOT-OH film was cut into a rectangular strip (2 cm × 0.5 cm), which was clamped with a stainless-steel tweezer for electrical connection. A 1 cm long strip was then immersed in electrolyte solution. A three-electrode electrochemical cell (Autolab PGSTAT204N Potentiostat) was used in which the strip served as the working electrode, a platinum net as the counter electrode, and Ag/AgCl in 3 M KCl as the reference electrode. A 0.1 M lithium perchlorate solution was used as the electrolyte. The potential was swept from −0.6 to +0.6 V at a scan rate of 5 mV/s for 200 times.

A three-electrode electrochemical cell as CV was used for stimulating the current of the RSF/PEDOT-OH film and gold plate (as control). A 0.1 M PBS (pH = 7.2) solution was used as electrolyte. Films were actuated by applying repeated pulses: −0.1 V for 1 ms, 0.1 V for 1 ms, and 0 V for 1 ms.

2.9. Adhesive Property. Ultrasonic cleaning is frequently used to assess the adhesion property between functional materials and matrix surface.[45] We used ultrasonic vibration with certain parameters (53 Hz, 187.5 W) in deionized water to compare the adhesive strengths of the RSF/PEDOT-OH film [modified at 30 mM monomer concentration, n(surfactant)/n(monomer) = 0.4, n(oxidant)/n(monomer) = 1.25, initial pH = 0.6] and PEDOT-OH which was deposited on an indium−tin oxide (ITO) glass slide by a typical electrochemical polymerization process (polymerized in 10 mM monomer dissolved in acetonitrile). Both samples were cut into rectangular strips (1 cm × 0.5 cm) for the tests.

2.10. Hydrophilicity Evaluation. Water contact angle (CA) measurement with water volume of 3 μL was performed using a CA goniometer (CA, OCA40 Micro, Dataphysics Ltd., Germany) to evaluate the hydrophilicity of hydrated RSF and modified films.

2.11. Biocompatibility Evaluation by Cell Culture in Vitro. Pheochromocytoma cells (PC12) were seeded with a density of 2 × 10^4 cells/well and cultivated in Roswell Park Memorial Institute (RPMI) 1640 medium supplemented with 1% penicillin−streptomycin solution, 15% horse serum, and 2.5% FBS in a humid incubator at 37 °C and 5% CO_2. Cell viabilities were analyzed by the 3-(4,5-dimethyl-2-thiazolyl)-2,5-diphenyl-2-*H*-tetrazolium bromide (MTT) method and expressed as a percentage of the RSF film without PEDOT-OH coating (100%).

PC12 were seeded on the RSF/PEDOT-OH film with a density of 1.5 × 10^4 cells/well and cultured for 3 days before the cell morphology was analyzed by SEM. For differentiation, the medium was diluted in half every day with a low serum medium (1% FBS) supplemented with NGF (50 ng mL^{-1}). Cells were fixed with 4% paraformaldehyde for 2 h at 4 °C. Then, the fixed samples were rinsed twice with PBS and dehydrated in a graded series of ethanol.[46] The dry samples were then sputtered with platinum and observed at a voltage of 10 kV by using a JSM-5600LV microscope.

The details of the MTT assay process and morphology evaluation can be found in the Supporting Information.

3. RESULTS AND DISCUSSION

3.1. Regulation of the Conductive Coating Morphology by Surfactant. Even though the hydroxymethyl unit of EDOT-OH improves its solubility in water, the hydrophobicity makes it difficult for the monomer to disperse in an aqueous environment. Thus, the polymer might preferentially form and agglomerate in solution rather than at the surface of the RSF film.[10] Because of the amphipathicity of surfactant, it is used to improve the solubility of the monomer and the interaction with RSF. As a surfactant, SDS has been used previously not only to increase the solubility and decrease the oxidation potential of EDOT or EDOT-OH during electrochemical deposition,[40,41,47,48] but also to influence the morphology, electrical properties, and mechanical properties of the resultant polymer.[45,49] The microstructure, morphology, and conductivity of PEDOT produced by chemical polymerization are also affected by SDS.[50,51] Therefore, in this work, SDS was adopted to improve the solubility of EDOT-OH and promote the in situ polymerization on the surface of the RSF film.

According to previous reports, SDS micelles can be produced in an aqueous environment and they display spherical, ellipsoidal, and rod morphology with the increase in concentration.[47,48,50] The critical micelle concentration (cmc) of SDS required to produce spherical micelles was reported to be 8 mmol L^{-1} at 25 °C.[52] There is no significant difference between the cmc at 25 °C and that at 30 °C, at which temperature we performed the polymerization.[53] Moreover, the addition of salt could further lower the cmc.[52] Therefore, the SDS concentrations of most systems in our work (higher than 8 mmol L^{-1}) are considered beyond the cmc. Compared to the system without amphipathic surfactant (Figure 1a), SDS at a higher concentration than cmc can form

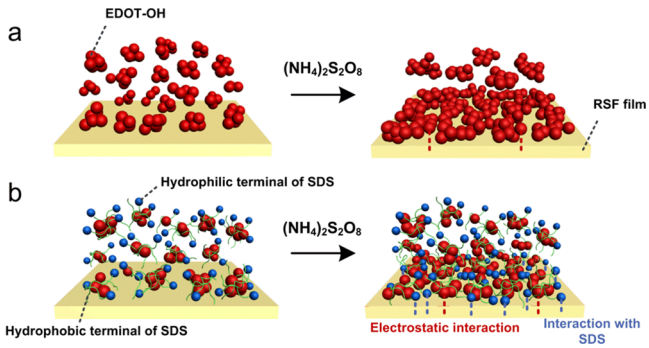

Figure 1. Illustration of the deposition of PEDOT-OH on the RSF film via in situ chemical oxidative polymerization (a) without and (b) with SDS as surfactant.

spherical micelles and come into contact with the monomers or polymers via lipophilic terminals while extending the hydrophilic terminals into water (Figure 1b) to improve the dispersion of monomers in water. After oxidation by APS, the monomers transformed to radical cations, which were attracted by the electronegative oxygen and nitrogen atoms of the peptide linkages in SF through electrostatic interaction primarily,[16] whereas the anion groups from C-terminus and amino acid residues of RSF had a similar interaction. After

DOI: 10.1021/acsami.8b13820
ACS Appl. Mater. Interfaces 2018, 10, 35547−35556

repetitive coupling,[37] PEDOT-OH was deposited on the surface of RSF as a CP coating. The presence of SDS micelles led to a relatively well-spread CP coating, which helped construct a conductive network on the surface of the RSF film. This improved the conductivity of the RSF/PEDOT-OH film. The dodecyl sulfate ions behaved as counterions for the PEDOT-OH. The electrostatic interaction was still crucial between RSF and doped PEDOT-OH which is rich in positive charge. At the same time, SDS micelles offered an added interaction between the hydrophilic RSF and hydrophobic PEDOT-OH, which made the linkage stronger.

It can be seen from the SEM images that the surface of ethanol-treated RSF film (Figure 2a) displayed a very smooth

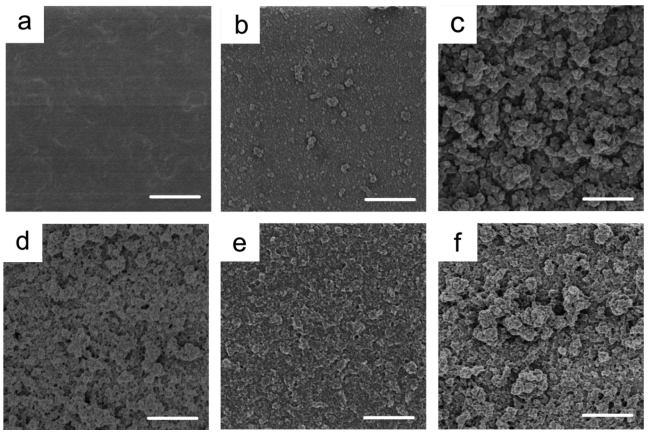

Figure 2. SEM images of the surface of the (a) RSF film and RSF/PEDOT-OH films with *n*(surfactant)/*n*(monomer) of (b) 0, (c) 0.1, (d) 0.3, (e) 0.4, and (f) 0.5. All scale bars represent 1 μm.

morphology, whereas the RSF/PEDOT-OH films displayed a relatively rough surface (Figure 2b–f). This result confirmed that PEDOT-OH was successfully deposited on the surface of the RSF film. In the case of the polymerization without SDS (Figure 2b), PEDOT-OH grew and was deposited as conventional particles for CP.[10] In the presence of SDS, EDOT-OH was well dispersed in solution and on the surface of the RSF film, and so was PEDOT-OH. As shown in Figure 2c–f, the addition of SDS micelles indeed led to a significant change in the morphology of the polymer coating, which provided the RSF/PEDOT-OH film with a better conductive network structure. With the increase in *n*(surfactant)/*n*(monomer) ratio, the coating spread was improved gradually and an optimum layer was obtained with the ratio of 0.4. As the *n*(surfactant)/*n*(monomer) ratio reached 0.5, some agglomerates of PEDOT-OH appeared again. Figure S1 shows a remarkable trend in the SEM images with a lower magnification. This was because the different SDS concentrations resulted in various micelle states. At the optimum dosage of SDS, the polymer coating displayed a smoother and well-organized morphology than the SDS-free film in our work. Similarly, it was also more ordered in comparison with the natural silk modified without SDS, which has obvious aggregation on the surface as reported.[16] This change in morphology was consistent with that of the PEDOT electrochemically polymerized in the presence of SDS.[47]

Figure 3a shows the influence of *n*(surfactant)/*n*(monomer) on R_s. The addition of SDS was beneficial for the conductivity of the composite. R_s decreased as the dosage of SDS increased and reached a minimum when the ratio was 0.4, which was

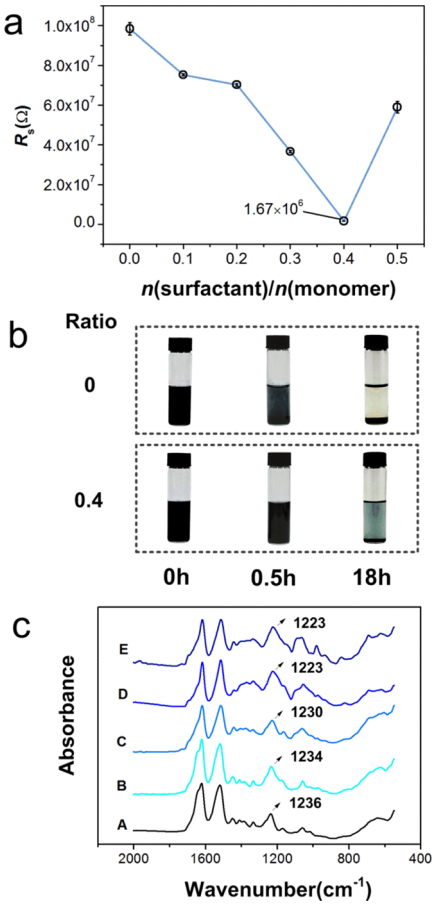

Figure 3. (a) Influence of *n*(surfactant)/*n*(monomer) on the R_s of the RSF/PEDOT-OH film. Circles represent the mean, whereas the error bar shows standard deviation (n = 5). (b) Photos of PEDOT-OH aqueous systems with or without SDS after polymerization at different standing times. (c) ATR–FTIR spectra of the (A) RSF film treated by water, (B) RSF film treated by SDS acid solution, (C) RSF/PEDOT-OH film without SDS, (D) RSF/PEDOT-OH film with SDS, and (E) RSF/PEDOT film with SDS.

attributed to the well-spread PEDOT-OH layer shown in Figure 2e. When the ratio increased to 0.5, R_s rose again because of the agglomerated PEDOT-OH. Detailed data of R_s and parameters of polymerization can be found in Table S1. These results confirmed that the smoothness and orderliness of the polymer coating was crucial for the conductivity of the RSF/PEDOT-OH composite. Similar results were reported in a previous work.[17] Thus, the surface morphology and conductance can be regulated by the dosage of surfactant to fabricate desired RSF/PEDOT-OH films.

During polymerization, black floccules of polymer with a larger size were found in the solution without SDS. On the contrary, the solution with SDS showed improved homogeneity. Figure 3b shows the influence of SDS on the dispersibility of PEDOT-OH in water. After standing for 0.5 h, the system without SDS faded more obviously, whereas more PEDOT-OH was dispersed in water in the presence of SDS after standing for 18 h. The system showed no marked change in color when the solution continued to stand. This also indicated that the surfactant played an important role in the construction of uniform PEDOT-OH. Figure 3c shows the FTIR spectra of different films. Compared to the RSF film treated by SDS acid solution (Figure 3c, curve B), the amide

DOI: 10.1021/acsami.8b13820
ACS Appl. Mater. Interfaces 2018, 10, 35547–35556

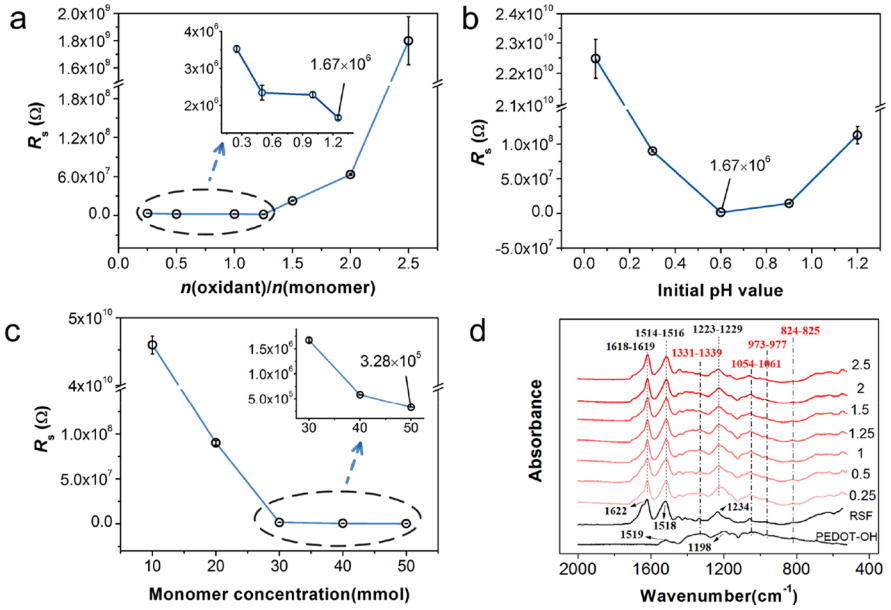

Figure 4. Influence of (a) n(oxidant)/n(monomer), (b) initial pH value, and (c) concentration of monomer on the R_s of the RSF/PEDOT-OH film. Circles represent the mean, whereas error bars show standard deviation (n = 5). (d) FTIR spectra of PEDOT-OH, RSF film, and RSF/PEDOT-OH films with different oxidant dosages.

III peak of the RSF/PEDOT-OH film without SDS (Figure 3c, curve C) moved to a lower wave number, which indicated the interaction between PEDOT-OH and RSF. In the presence of SDS [n(surfactant)/n(monomer) = 0.4], the peak was shifted much further (Figure 3c, curve D). The first reason for this effect is that the SDS facilitates additional interaction between the PEDOT-OH conductive coating and RSF, which is critical for the product. In addition, the transmission spectra obtained with the KBr pellet method showed that the absorption peak of SDS at 1220 cm^{-1} affected the resultant peak position of amide III, which was shifted from 1235 to 1225 cm^{-1} (Figure S2). However, this influence was not observed from the ATR spectra (Figure 3c, curve A, B). Therefore, the overlap of peaks of SDS may be considered as another reason for the shift of the peak position. Compared to the RSF film with a PEDOT conductive coating with SDS (Figure 3c, curve E), the hydroxymethyl group made little difference to the peak position of amide III of RSF (Figure 3c, curve D).

3.2. Influence of the Dosage of Oxidant and Initial pH Value. Generally, lack of oxidant may result in an incomplete polymerization and lead to residual monomers. On the other hand, peroxidation could occur in the presence of excess oxidant. Usually, each monomer consumes one equivalent of APS (two equivalents for a single electron oxidant) to form undoped polythiophene. Then, every third or fourth thiophene moiety loses one electron to the additional APS to form a doped state.[37] Therefore, about 0.125 to 0.17 additional equivalents of APS were needed for efficient doping. Experimental results may vary around the theoretical value. The influence of n(oxidant)/n(monomer) on R_s is shown in Figure 4a (more detailed R_s data and parameters of polymerization are given in Table S2). It can be seen that R_s reached the optimum value when the ratio was 1.25. R_s increased significantly from the minimum value when the ratio exceeded 1.25 because of the peroxidation caused by the presence of excess APS. Moreover, the decrease in the APS amount had little effect on the R_s even though the resulting RSF/PEDOT-OH film was less thick. The generated PEDOT-OH was probably enough to construct the conductive coating. This phenomenon is beneficial for fabricating a relatively thin and transparent composite which utilizes the transparency of doped PEDOT and its derivatives.

Figure 4d shows the ATR−FTIR spectra of the RSF film after it was treated by SDS acid solution and RSF/PEDOT-OH films with different oxidant dosages. Compared to the RSF film, the RSF/PEDOT-OH films showed relatively stronger characteristic peaks of PEDOT derivative at about 1328 cm^{-1} (C−C or C═C flexing vibration), 1050 cm^{-1} (C−O−C deformation vibration), 965 and 824 cm^{-1} (C−S−C deformation vibration). Peaks at 1198 cm^{-1} (C−O−C stretching vibration) and 1519 cm^{-1} (C═C stretching vibration) showed some overlap with RSF.[16,54−56] It should be noted that the peak intensity was stronger when the ratio was around 1.25, which explained the influence of optimal oxidant dosage. In addition, compared with the RSF film, the peaks for amide I, amide II, and amide III in the RSF/PEDOT-OH films all shifted to a lower wave number. Furthermore, the broad peak of amide I of RSF became sharper after modification. All these data indicate that there are indeed some interactions between PEDOT-OH and the peptide linkages of SF macromolecular chains as reported by Xia and Lu.[16]

The initial pH value of the system is also considered an important parameter during the chemical oxidative polymerization of PEDOT according to previous research.[57] The influence of the initial pH value on R_s is shown in Figure 4b. More detailed R_s data and parameters of polymerization are given in Table S3.

It can be seen that the optimal initial pH value was 0.6, which means that this reaction preferred strong acidic conditions. This might be because hydrogen ions promoted the generation of intermediate dimers or trimers,[37] which accelerated the polymerization. Under alkaline conditions, the generation of intermediate dimers (or trimers) was inhibited and so was the polymerization. The large number of radical cations during the first stage of in situ polymerization might be

DOI: 10.1021/acsami.8b13820
ACS Appl. Mater. Interfaces 2018, 10, 35547−35556

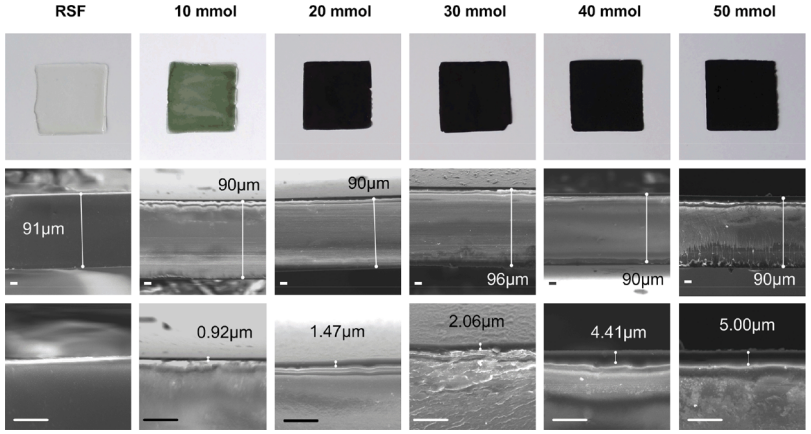

Figure 5. Digital photos and SEM images of cross sections of the RSF film and RSF/PEDOT-OH films with different monomer concentrations. All scale bars represent 10 μm.

an important condition for the formation of conductive coating of the RSF/PEDOT-OH film. Figure S3 shows that the final pH value of the system was always lower than the initial one because of the protons generated during polymerization. In the system with initial pH value of 10, the solution displayed a more transparent and lighter color after polymerization for 24 h, which indicated that only a small quantity of oligomer was generated (Figure S4). Moreover, the solution became acidic (pH = 2.9). This phenomenon demonstrated that the polymerization could still be initiated under alkaline conditions; however, the process was not as intense as that with a lower initial pH value.

With regard to the systems in which the initial pH value was lower than 0.6, more dimers or trimers were generated in the early stage of the reaction because of the effect of a number of hydrogen ions. This is consistent with the experimental observation that the color of the system became darker earlier with a lower pH value, which indicated that the polymers were formed sooner. A certain amount of monomer in the solution would result in a lower average molecular chain length of formed CP because of the presence of more polymers with a relatively low MW. Consequently, R_s was larger at a lower pH value than the optimum pH because of the conductive gaps derived from polymers with a relatively low MW.

3.3. Regulation of Conductive Coating Thickness by Monomer Concentration. It is obvious that the concentration of monomer can affect the conductivity of the RSF/PEDOT-OH film, and, thus, this factor was investigated next. The influence of the monomer concentration on R_s is shown in Figure 4c. The curve dropped obviously at first and became almost flat at the end. Thus, 50 mmol L^{-1} can be regarded as the optimal monomer concentration in the range of our experiment. More detailed R_s data and parameters of polymerization are given in Table S4.

As seen from the digital photos (Figure 5), the RSF film became black after modification and lost transparency gradually along with the increase in concentration of the monomer. The SEM images of cross sections reveal black regions of conductive layers on both sides of the film and a silk layer in the center after modification. The thickness of the conductive layer ranged from 0.92 to 5 μm, which is much thinner than that of the Ppy conductive layer previously reported.[8] This might be beneficial for the fabrication of a transparent film. The layer on one side was slightly thicker than that on the other side because of the effect of gravity on the upper and bottom surfaces of the silk film. Moreover, the layer became thicker progressively along with the increase in concentration of the monomer (Figure 5). As the concentration exceeded 50 mmol L^{-1}, the excess monomers had little impact on the formation of the conductive layer. The thickness of the conductive layer with 50 mmol L^{-1} monomer concentration was 5 μm, which corresponded to an R_s of 3.28×10^{-5} Ω or a conductance of 6.1×10^{-3} S/cm. Considering the difference in calculation methods, the conductance of the RSF/PEDOT-OH film is slightly lower than that of modified silk by in situ chemical polymerization of PEDOT.[16] Similarly, silk modified by in situ chemical-polymerized Pani and Ppy also shows a higher conductivity.[16,17] This is probably attributed to the lack of a hierarchical fibrillar structure present in the natural silks. However, the shape and structure of RSF materials are more tunable than natural silks. The conductive SF base on blending or dipping of Pani, and PEDOT:PSS perform better conductivity ($\sim 10^{-2}$ to 10^{0} S/cm).[18,21,22] To achieve this conductivity, the blending process needs high contents of CPs, which are not biodegradable and have side effects for further implantation. The dipping process used for natural silk modification may be not feasible for RSF material, as it is difficult to obtain a stable interface between the conductive layer and the RSF layer. The higher monomer concentration resulted in deposition of more CP, which led to a thicker conductive layer. Furthermore, the conductivity of PEDOT-OH followed the classical relationship: the conductivity performed at a much lower value when the layer was very thin but saturated to a constant value when the layer reached a thickness that is enough to provide the conductive path.[58,59] Thus, R_s decreased with the increase in monomer concentration and reached a stable plateau at 50 mmol L^{-1}. Moreover, the higher monomer concentration also resulted in the deposition of a denser CP, which benefitted the construction of a well-organized conductive coating. The peak of amide III in ATR−FTIR spectra of the RSF/PEDOT-OH film shifted to a lower wave number with a higher monomer concentration, which indicated a more intense interaction (Figure S5). Thus, the thickness and related conductance can be regulated by the monomer concentration, which is also a method to control the structure of the RSF/PEDOT-OH film.

3.4. Electrochemical Characterization, Surface Properties, and Biocompatibility Evaluation. On the basis of various in vivo applications of conductive biomaterials, the electrochemical performance, surface properties, and bio-

DOI: 10.1021/acsami.8b13820
ACS Appl. Mater. Interfaces 2018, 10, 35547−35556

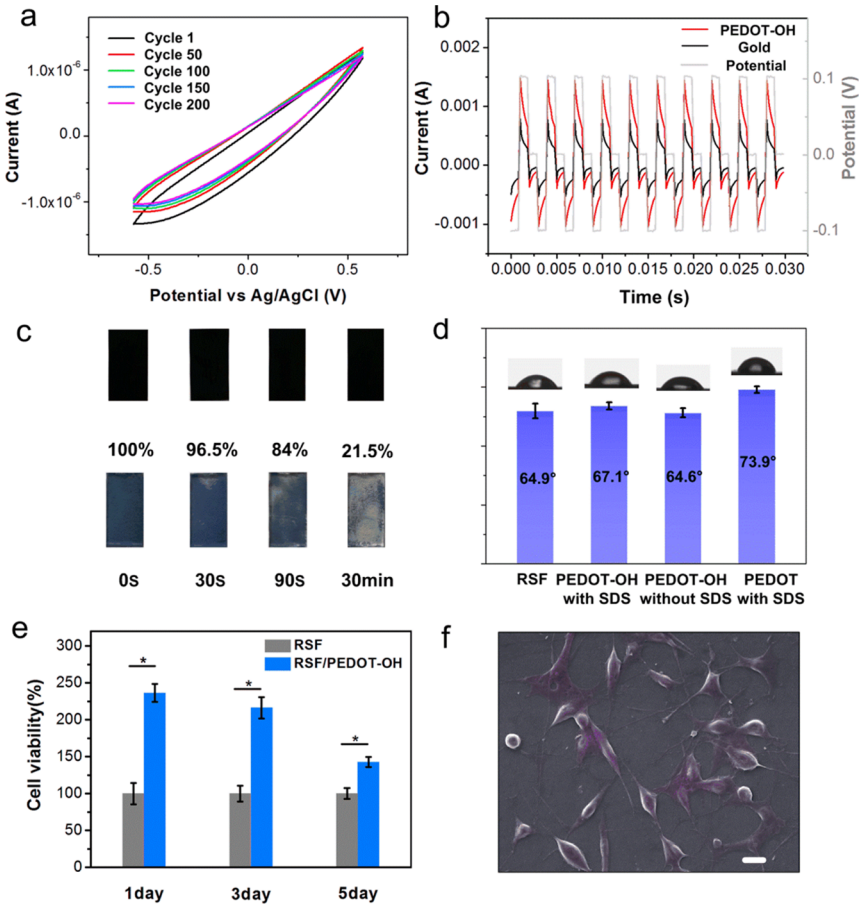

Figure 6. (a) Cyclic voltammograms of the RSF/PEDOT-OH film. (b) Actuation performance of RSF/PEDOT-OH under potential pulse. (c) Digital photos of the RSF/PEDOT-OH film (first line) and ITO/PEDOT-OH (second line) after ultrasonic cleaning for different durations. The remaining area percentage of PEDOT-OH on ITO is indicated above the ITO/PEDOT-OH photos. (d) CAs for different films. (e) Cell viability of PC12 cultured for 5 days (*$P < 0.05$). (f) Morphology and spreading (SEM) of PC12 cultured under NGF for 3 days on the RSF/PEDOT-OH film. The scale bar represents 10 μm.

compatibility of RSF/PEDOT-OH films were investigated. We initially evaluated the electrochemical stability by subjecting the materials to 200 oxidation and reduction cycles using CV (Figure 6a). The CV curve of RSF/PEDOT-OH displayed no distinct oxidation or reduction peaks. At the same time, the curve showed good symmetry, which indicated that the RSF/PEDOT-OH materials had good reversibility. After 50 cycles, the response current increased significantly, suggesting that the electrolyte concentration in the film reached a steady state after a few cycles. After 200 cycles, the curve maintained a similar shape. The stored charge decreased slightly and the film retained 84% of its initial charge storage capacity (Figure S6). During a constant voltage pulse, the RSF/PEDOT-OH exhibited a distinct and stable response current (Figure 6b), as the charge delivered during the pulse is equal to the time integral of the current. It was found that the RSF/PEDOT-OH film had better charge storage ability than the gold plate. Overall, the RSF/PEDOT-OH material had favorable electrochemical stability and charge storage performance, indicating its potential for applications in long-term implants or biosensors.

As seen from Figure 6c, after ultrasonic cleaning for 30 min, the conductive coating of the RSF/PEDOT-OH film showed no significant change. On the other hand, the film that was electrochemically polymerized on ITO dissolved rapidly during the cleaning and very little of the film was left in the end. In addition, we also found that there was no significant change in the conductance of the RSF/PEDOT-OH film after ultrasonic cleaning for 30 min, whereas the conductance changed obviously without SDS (data not shown). This result indicates that SDS endowed RSF/PEDOT-OH with good fastness, which made it suitable for certain application environments, such as in vivo. Figure 6d shows that the hydroxymethyl group contributed significantly to the hydrophilicity of film surface, whereas SDS had little influence. The RSF/PEDOT-OH film had a similar hydrophilicity as that of RSF.

Figure 6e shows the results of cell proliferation of PC12 cultured on the RSF/PEDOT-OH film and RSF film for 5 days, respectively. Compared to the RSF film, the cell viability of the RSF/PEDOT-OH film was higher on each of the days, which suggested that the RSF/PEDOT-OH film had better biocompatibility. The PEDOT-OH layer may contribute more to the increase in roughness, which is beneficial for the adhesion of cells. Furthermore, the cell morphology and spreading were observed by SEM (Figure 6f). According to the SEM images, PC12 was adhered and well spread on the RSF/PEDOT-OH film. Guided by NGF, a distinct PC12 differentiation was observed and the axons' length of PC12 was more than 20 μm. Both evaluations indicated that the RSF/PEDOT-OH film has good biocompatibility and potential for biomedical applications.

DOI: 10.1021/acsami.8b13820
ACS Appl. Mater. Interfaces 2018, 10, 35547−35556

4. CONCLUSIONS

In this study, a biocompatible RSF/PEDOT-OH film electrode was fabricated through an in situ chemical oxidative polymerization in aqueous conditions. The hydroxymethyl derivative was adopted as EDOT monomer to provide more dispersibility, hydrophilicity, and further functional possibilities for biomedical applications. To construct a superior conductive coating, SDS was added to the system, which improved the dispersion of the monomer and polymer, and caused a stronger interaction between PEDOT-OH and RSF. As a result, a well-organized and stable PEDOT-OH coating was obtained, which provided improved conductivity and fastness of the RSF/PEDOT-OH film. The optimum dosage of surfactant to achieve a uniform film morphology was n(surfactant)/n(monomer) = 0.4. At the same time, an excess of oxidant caused peroxidation, which led to lower conductivity, whereas the lack of oxidant had limited influence. Also, the reaction preferred strong acidic conditions. The thickness and conductivity of the PEDOT-OH conductive layer increased along with the concentration of the monomer, and gradually reached a plateau at 50 mmol L^{-1}. At the monomer concentration of 50 mmol L^{-1}, n(surfactant)/n(monomer) = 0.4, and n(oxidant)/n(monomer) = 1.25, the thickness of the conductive layer was 5 μm and the R_s was 3.28×10^5, corresponding to the conductivity of 6.1×10^{-3} S/cm. The conductivity may be further improved by adjusting the doping agent and the microstructure of PEDOT-OH. A conductive RSF film with higher transparency is expected to be achieved for broader applications through the construction of a thinner CP coating. Furthermore, the RSF/PEDOT-OH film exhibited good electrochemical stability and fastness under ultrasonic cleaning and better biocompatibility than the pure RSF film. This material is promising for bioelectrical applications, such as nonirritant sensors on the body surface or implanted sensors to monitor health signals, bioelectronic devices for drug delivery and diagnostics, and tissue engineering scaffolds for nerve regeneration.

■ ASSOCIATED CONTENT

Supporting Information

The Supporting Information is available free of charge on the ACS Publications website at DOI: 10.1021/acsami.8b13820.

MTT assay procedure, the surface morphology of the PEDOT-OH/RSF composite films in lower magnification (SEM), the FTIR spectra of SDS, acid-treated RSF with and without SDS, change of pH value of polymerization systems with different initial pH values, digital photos of solutions after polymerization, ATR–FTIR spectra of the RSF/PEDOT-OH film with different monomer concentrations, recipes of polymerization with different dosages of surfactant, recipes of polymerization with different dosages of oxidant, recipes of polymerization with different pH values, recipes of polymerization with different monomer concentrations, and detailed R_s values (PDF)

■ AUTHOR INFORMATION

Corresponding Authors

*E-mail: bozhu@shu.edu.cn (B.Z.).
*E-mail: zyp@dhu.edu.cn (Y.Z.).

ORCID

Ao Zhuang: 0000-0002-9531-4031
Suna Fan: 0000-0001-6508-360X
Yaopeng Zhang: 0000-0002-7175-6150

Author Contributions

Y.Z. and B.Z. directed the project. A.Z. performed most of the experiments and wrote the paper. Y.B. synthesized EDOT-OH. J.Z. assisted A.Z. to observe the morphology of films. S.F. contributed to the electrochemical experiment design and analysis of the result. H.S. directed the biocompatibility characterization. X.H. contributed to the analysis of the polymerization mechanism. All authors have given approval to the final version of the paper.

Notes

The authors declare no competing financial interest.

■ ACKNOWLEDGMENTS

This work is supported by the National Natural Science Foundation of China (21674018), the National Key Research and Development Program of China (2018YFC1105802/2018YFC1105800), the Fundamental Research Funds for the Central Universities (CUSF-DH-D-2018011), the National Key Research and Development Program of China (2016YFA0201702, 2018YFC1106002), and the "Shuguang Program" supported by Shanghai Education Development Foundation and Shanghai Municipal Education Commission (15SG30). B.Z. acknowledges financial support from the National Natural Science Foundation of China (21474014) and the Natural Science Foundation of Shanghai (14ZR1400200).

■ ABBREVIATIONS

EDOT-OH, hydroxymethyl-3,4-ethylenedioxythiophene; RSF, regenerated silk fibroin; APS, ammonium persulfate; SEM, scanning electron microscope; PEDOT-OH, poly(hydroxymethyl-3,4-ethylenedioxythiophene); FTIR, Fourier transform infrared spectroscopy; SF, silk fibroin; CPs, conductive polymers; Ppy, polypyrrole; *Pani*, polyaniline; PEDOT, poly(3,4-ethylenedioxythiophene); PBS, phosphate buffer saline; NGF, nerve growth factor; ITO, indium–tin oxide; EDOT, 3,4-ethylenedioxythiophene; cmc, critical micelle concentration

■ REFERENCES

(1) van den Brand, R.; Heutschi, J.; Barraud, Q.; DiGiovanna, J.; Bartholdi, K.; Huerlimann, M.; Friedli, L.; Vollenweider, I.; Moraud, E. M.; Duis, S.; Dominici, N.; Micera, S.; Musienko, P.; Courtine, G. Restoring Voluntary Control of Locomotion after Paralyzing Spinal Cord Injury. *Science* **2012**, *336*, 1182–1185.

(2) O'Doherty, J. E.; Lebedev, M. A.; Ifft, P. J.; Zhuang, K. Z.; Shokur, S.; Bleuler, H.; Nicolelis, M. A. L. Active Tactile Exploration Using a Brain-Machine-Brain Interface. *Nature* **2011**, *479*, 228–231.

(3) Aflalo, T.; Kellis, S.; Klaes, C.; Lee, B.; Shi, Y.; Pejsa, K.; Shanfield, K.; Hayes-Jackson, S.; Aisen, M.; Heck, C.; Liu, C.; Andersen, R. A. Decoding Motor Imagery from the Posterior Parietal Cortex of a Tetraplegic Human. *Science* **2015**, *348*, 906–910.

(4) Moschou, E. A.; Peteu, S. F.; Bachas, L. G.; Madou, M. J.; Daunert, S. Artificial Muscle Material with Fast Electroactuation under Neutral pH Conditions. *Chem. Mater.* **2004**, *16*, 2499–2502.

(5) Kim, D.-H.; Viventi, J.; Amsden, J. J.; Xiao, J.; Vigeland, L.; Kim, Y.-S.; Blanco, J. A.; Panilaitis, B.; Frechette, E. S.; Contreras, D.; Kaplan, D. L.; Omenetto, F. G.; Huang, Y.; Hwang, K.-C.; Zakin, M. R.; Litt, B.; Rogers, J. A. Dissolvable Films of Silk Fibroin for Ultrathin Conformal Bio-Integrated Electronics. *Nat. Mater.* **2010**, *9*, 511–517.

DOI: 10.1021/acsami.8b13820
ACS Appl. Mater. Interfaces 2018, 10, 35547–35556

(6) Pal, R. K.; Farghaly, A. A.; Wang, C.; Collinson, M. M.; Kundu, S. C.; Yadavalli, V. K. Conducting Polymer-Silk Biocomposites for Flexible and Biodegradable Electrochemical Sensors. *Biosens. Bioelectron.* **2016**, *81*, 294−302.
(7) Gao, W.; Emaminejad, S.; Nyein, H. Y. Y.; Challa, S.; Chen, K.; Peck, A.; Fahad, H. M.; Ota, H.; Shiraki, H.; Kiriya, D.; Lien, D.-H.; Brooks, G. A.; Davis, R. W.; Javey, A. Fully Integrated Wearable Sensor Arrays for Multiplexed in Situ Perspiration Analysis. *Nature* **2016**, *529*, 509−514.
(8) Romero, I. S.; Schurr, M. L.; Lally, J. V.; Kotlik, M. Z.; Murphy, A. R. Enhancing the Interface in Silk-Polypyrrole Composites through Chemical Modification of Silk Fibroin. *ACS Appl. Mater. Interfaces* **2013**, *5*, 553−564.
(9) Romero, I. S.; Bradshaw, N. P.; Larson, J. D.; Severt, S. Y.; Roberts, S. J.; Schiller, M. L.; Leger, J. M.; Murphy, A. R. Biocompatible Electromechanical Actuators Composed of Silk-Conducting Polymer Composites. *Adv. Funct. Mater.* **2014**, *24*, 3866−3873.
(10) Severt, S. Y.; Ostrovsky-Snider, N. A.; Leger, J. M.; Murphy, A. R. Versatile Method for Producing 2D and 3D Conductive Biomaterial Composites Using Sequential Chemical and Electrochemical Polymerization. *ACS Appl. Mater. Interfaces* **2015**, *7*, 25281−25288.
(11) Larson, J. D.; Fengel, C. V.; Bradshaw, N. P.; Romero, I. S.; Leger, J. M.; Murphy, A. R. Enhanced Actuation Performance of Silk-Polypyrrole Composites. *Mater. Chem. Phys.* **2017**, *186*, 67−74.
(12) Severt, S. Y.; Maxwell, S. L.; Bontrager, J. S.; Leger, J. M.; Murphy, A. R. Mimicking Muscle Fiber Structure and Function through Electromechanical Actuation of Electrospun Silk Fiber Bundles. *J. Mater. Chem. B* **2017**, *5*, 8105−8114.
(13) Bhadani, S. N.; Kumari, M.; Gupta, S. K. S.; Sahu, G. C. Preparation of Conducting Fibers via the Electrochemical Polymerization of Pyrrole. *J. Appl. Polym. Sci.* **1997**, *64*, 1073−1077.
(14) Cucchi, I.; Boschi, A.; Arosio, C.; Bertini, F.; Freddi, G.; Catellani, M. Bio-Based Conductive Composites: Preparation and Properties of Polypyrrole (Ppy)-Coated Silk Fabrics. *Synth. Met.* **2009**, *159*, 246−253.
(15) Hosseini, S. H.; Pairovi, A. Preparation of Conducting Fibres from Cellulose and Silk by Polypyrrole Coating. *Iran. Polym. J.* **2005**, *14*, 934−940.
(16) Xia, Y.; Lu, Y. Fabrication and Properties of Conductive Conjugated Polymers/Silk Fibroin Composite Fibers. *Compos. Sci. Technol.* **2008**, *68*, 1471−1479.
(17) Xia, Y.; Lu, X.; Zhu, H. Natural Silk Fibroin/Polyaniline (Core/Shell) Coaxial Fiber: Fabrication and Application for Cell Proliferation. *Compos. Sci. Technol.* **2013**, *77*, 37−41.
(18) Zhang, J.; Qiu, K.; Sun, B.; Fang, J.; Zhang, K.; EI-Hamshary, H.; Al-Deyab, S. S.; Mo, X. The Aligned Core-Sheath Nanofibers with Electrical Conductivity for Neural Tissue Engineering. *J. Mater. Chem. B* **2014**, *2*, 7945−7954.
(19) Ismail, Y. A.; Martínez, J. G.; Otero, T. F. Fibroin/Polyaniline Microfibrous Mat. Preparation and Electrochemical Characterization as Reactive Sensor. *Electrochim. Acta* **2014**, *123*, 501−510.
(20) Shi, Y.; Li, Z.; Shi, J.; Zhang, F.; Zhou, X.; Li, Y.; Holmes, M.; Zhang, W.; Zou, X. Titanium Dioxide-Polyaniline/Silk Fibroin Microfiber Sensor for Pork Freshness Evaluation. *Sens. Actuators, B* **2018**, *260*, 465−474.
(21) Irwin, M. D.; Roberson, D. A.; Olivas, R. I.; Wicker, R. B.; MacDonald, E. Conductive Polymer-Coated Threads as Electrical Interconnects in E-Textiles. *Fibers Polym.* **2011**, *12*, 904−910.
(22) Tsukada, S.; Nakashima, H.; Torimitsu, K. Conductive Polymer Combined Silk Fiber Bundle for Bioelectrical Signal Recording. *PLoS One* **2012**, *7*, No. e33689.
(23) Müller, C.; Hamedi, M.; Karlsson, R.; Jansson, R.; Marcilla, R.; Hedhammar, M.; Inganäs, O. Woven Electrochemical Transistors on Silk Fibers. *Adv. Mater.* **2011**, *23*, 898−901.
(24) Shen, Y.; Johnson, M. A.; Martin, D. C. Microstructural Characterization of Bombyx Mori Silk Fibers. *Macromolecules* **1998**, *31*, 8857−8864.
(25) Ling, S.; Qin, Z.; Li, C.; Huang, W.; Kaplan, D. L.; Buehler, M. J. Polymorphic Regenerated Silk Fibers Assembled through Bioinspired Spinning. *Nat. Commun.* **2017**, *8*, 1387.
(26) Jin, H.-J.; Kaplan, D. L. Mechanism of Silk Processing in Insects and Spiders. *Nature* **2003**, *424*, 1057−1061.
(27) Cogan, S. F. Neural Stimulation and Recording Electrodes. *Annu. Rev. Biomed. Eng.* **2008**, *10*, 275−309.
(28) Wilks, S. J.; Richardson-Burns, S. M.; Hendricks, J. L.; Martin, D. C.; Otto, K. J. Poly(3,4-ethylenedioxythiophene) as a Micro-Neural Interface Material for Electrostimulation. *Front. Neuroeng.* **2009**, *2*, 7.
(29) Discher, D. E.; Janmey, P.; Wang, Y.-L. Tissue Cells Feel and Respond to the Stiffness of Their Substrate. *Science* **2005**, *310*, 1139−1143.
(30) Mitragotri, S.; Lahann, J. Physical Approaches to Biomaterial Design. *Nat. Mater.* **2009**, *8*, 15−23.
(31) Xie, C.; Liu, J.; Fu, T.-M.; Dai, X.; Zhou, W.; Lieber, C. M. Three-Dimensional Macroporous Nanoelectronic Networks as Minimally Invasive Brain Probes. *Nat. Mater.* **2015**, *14*, 1286−1292.
(32) Minev, I. R.; Musienko, P.; Hirsch, A.; Barraud, Q.; Wenger, N.; Moraud, E. M.; Gandar, J.; Capogrosso, M.; Milekovic, T.; Asboth, L.; Torres, R. F.; Vachicouras, N.; Liu, Q.; Pavlova, N.; Duis, S.; Larmagnac, A.; Voros, J.; Micera, S.; Suo, Z.; Courtine, G.; Lacour, S. P. Electronic Dura Mater for Long-Term Multimodal Neural Interfaces. *Science* **2015**, *347*, 159−163.
(33) Shtein, Z.; Shoseyov, O. When Bottom-Up Meets Top-Down. *Proc. Natl. Acad. Sci. U.S.A.* **2017**, *114*, 428−429.
(34) Yang, Y.; Ding, F.; Wu, J.; Hu, W.; Liu, W.; Liu, J.; Gu, X. Development and Evaluation of Silk Fibroin-Based Nerve Grafts Used for Peripheral Nerve Regeneration. *Biomaterials* **2007**, *28*, 5526−5535.
(35) Marelli, B.; Patel, N.; Duggan, T.; Perotto, G.; Shirman, E.; Li, C.; Kaplan, D. L.; Omenetto, F. G. Programming Function into Mechanical Forms by Directed Assembly of Silk Bulk Materials. *Proc. Natl. Acad. Sci. U.S.A.* **2017**, *114*, 451−456.
(36) Asplund, M.; Nyberg, T.; Inganäs, O. Electroactive Polymers for Neural Interfaces. *Polym. Chem.* **2010**, *1*, 1374−1391.
(37) Elshchner, A.; Kirchmeyer, S.; Lovenich, W.; Merker, U.; Reuter, K. *PEDOT: Principles and Applications of an Intrinsically Conductive Polymer*; Wiley, 2011; p 165.
(38) Luo, S.-C.; Sekine, J.; Zhu, B.; Zhao, H.; Nakao, A.; Yu, H.-h. Polydioxythiophene Nanodots, Nonowires, Nano-Networks, and Tubular Structures: The Effect of Functional Groups and Temperature in Template-Free Electropolymerization. *ACS Nano* **2012**, *6*, 3018−3026.
(39) Green, R. A.; Lovell, N. H.; Poole-Warren, L. A. Cell Attachment Functionality of Bioactive Conducting Polymers for Neural Interfaces. *Biomaterials* **2009**, *30*, 3637−3644.
(40) Luo, S.-C.; Ali, E. M.; Tansil, N. C.; Yu, H.-h.; Gao, S.; Kantchev, E. A. B.; Ying, J. Y. Thin, Ultrasmooth, and Functionalized PEDOT Films with In Vitro and In Vivo Biocompatibility. *Langmuir* **2008**, *24*, 8071−8077.
(41) Lu, Y.; Wen, Y.-p.; Lu, B.-y.; Duan, X.-m.; Xu, J.-k.; Zhang, L.; Huang, Y. Electrosynthesis and Characterization of Poly(Hydroxy-Methylated-3,4-Ethylenedioxythiophene) Film in Aqueous Micellar Solution and Its Biosensing Application. *Chin. J. Polym. Sci.* **2012**, *30*, 824−836.
(42) Lima, A.; Schottland, P.; Sadki, S.; Chevrot, C. Electropolymerization of 3,4-Ethylenedioxythiophene and 3,4-Ethylenedioxythiophene Methanol in the Presence of Dodecylbenzenesulfonate. *Synth. Met.* **1998**, *93*, 33−41.
(43) Xiao, Y.; Cui, X.; Hancock, J. M.; Bouguettaya, M.; Reynolds, J. R.; Martin, D. C. Electrochemical Polymerization of Poly-(Hydroxymethylated-3,4-Ethylenedioxythiophene) (PEDOT-Meoh) on Multichannel Neural Probes. *Sens. Actuators, B* **2004**, *99*, 437−443.
(44) Ha, S.-W.; Tonelli, A. E.; Hudson, S. M. Structural Studies of Bombyx mori Silk Fibroin during Regeneration From Solutions and Wet Fiber Spinning. *Biomacromolecules* **2005**, *6*, 1722−1731.

DOI: 10.1021/acsami.8b13820
ACS Appl. Mater. Interfaces 2018, 10, 35547−35556

(45) Wu, X.; Pei, W.; Zhang, H.; Chen, Y.; Guo, X.; Chen, H.; Wang, S. Sodium Dodecyl Sulfate Doping PEDOT to Enhance the Performance of Neural Microelectrode. *J. Electroanal. Chem.* **2015**, *758*, 26−32.
(46) Li, Z.; Liu, Q.; Wang, H.; Song, L.; Shao, H.; Xie, M.; Xu, Y.; Zhang, Y. Bladder Acellular Matrix Graft Reinforced Silk Fibroin Composite Scaffolds Loaded VEGF with Aligned Electrospun Fibers in Multiple Layers. *ACS Biomater. Sci. Eng.* **2015**, *1*, 238−246.
(47) Sakmeche, N.; Aaron, J. J.; Fall, M.; Aeiyach, S.; Jouini, M.; Lacroix, J. C.; Lacaze, P. C. Anionic Micelles; a New Aqueous Medium for Electropolymerization of Poly(3,4-Ethylenedioxythiophene) Films on Pt Electrodes. *Chem. Commun.* **1996**, 2723−2724.
(48) Sakmeche, N.; Bazzaoui, E. A.; Fall, M.; Aeiyach, S.; Jouini, M.; Lacroix, J. C.; Aaron, J. J.; Lacaze, P. C. Application of Sodium Dodecylsulfate (SDS) Micellar Solution as an Organized Medium for Electropolymerization of Thiophene Derivatives in Water. *Synth. Met.* **1997**, *84*, 191−192.
(49) Lyutov, V.; Gruia, V.; Efimov, I.; Bund, A.; Tsakova, V. An Acoustic Impedance Study of PEDOT Layers Obtained in Aqueous Solution. *Electrochim. Acta* **2016**, *190*, 285−293.
(50) Han, M. G.; Foulger, S. H. Facile Synthesis of Poly(3,4-ethylenedioxythiophene) Nanofibers from an Aqueous Surfactant Solution. *Small* **2006**, *2*, 1164−1169.
(51) Eren, E.; Celik, G.; Uygun, A.; Tabačiarová, J.; Omastová, M. Synthesis of Poly(3,4-Ethylenedioxythiophene)/Titanium Dioxide Nanocomposites in the Presence of Surfactants and Their Properties. *Synth. Met.* **2012**, *162*, 1451−1458.
(52) Zhao, J.; Fung, B. M. NMR Study of the Transformation of Sodium Dodecyl Sulfate Micelles. *Langmuir* **1993**, *9*, 1228−1231.
(53) Lv, J. X. *Investigation on the Aggregation Behavior and Mechanism of Surfactant SDS Micelle*; Dalian University: China, 2006.
(54) Garreau, S.; Louarn, G.; Buisson, J. P.; Froyer, G.; Lefrant, S. In Situ Spectroelectrochemical Raman Studies of Poly(3,4-ethylenedioxythiophene) (PEDT). *Macromolecules* **1999**, *32*, 6807−6812.
(55) Han, M. G.; Foulger, S. H. Crystalline Colloidal Arrays Composed of Poly(3,4-ethylenedioxythiophene)-Coated Polystyrene Particles with a Stop Band in the Visible Regime. *Adv. Mater.* **2004**, *16*, 231−234.
(56) Wang, M.; Kovacik, P.; Gleason, K. K. Chemical Vapor Deposition of Thin, Conductive, and Fouling-Resistant Polymeric Films. *Langmuir* **2017**, *33*, 10623−10631.
(57) Wang, J.; Cai, G.; Zhu, X.; Zhou, X. Oxidative Chemical Polymerization of 3, 4-Ethylenedioxythiophene and Its Applications in Antistatic Coatings. *J. Appl. Polym. Sci.* **2012**, *124*, 109−115.
(58) Ha, Y.-H.; Nikolov, N.; Pollack, S. K.; Mastrangelo, J.; Martin, B. D.; Shashidhar, R. Towards a Transparent, Highly Conductive Poly(3,4-Ethylenedioxythiophene). *Adv. Funct. Mater.* **2004**, *14*, 615−622.
(59) Zhang, X.-G.; Butler, W. H. Conductivity of Metallic-Films and Multilayers. *Phys. Rev. B: Condens. Matter Mater. Phys.* **1995**, *51*, 10085−10103.

DOI: 10.1021/acsami.8b13820
ACS Appl. Mater. Interfaces 2018, 10, 35547−35556